

# Lawrence Berkeley National Laboratory

LBL Publications

## Title

Controlling the Temperature and Speed of the Phase Transition of VO<sub>2</sub> Microcrystals

## Permalink

<https://escholarship.org/uc/item/0vc6b3gr>

## Journal

ACS Applied Materials & Interfaces, 8(3)

## ISSN

1944-8244

## Authors

Yoon, Joonseok

Kim, Howon

Chen, Xian

et al.

## Publication Date

2016-01-27

## DOI

10.1021/acsami.5b11144

Peer reviewed

# Controlling phase transition temperature and speed of VO<sub>2</sub> micro-single crystal

*Joonseok Yoon, Howon Kim, Giyong Lee, Xian Chen, Nobumichi Tamura, Bongjin Simon Mun, \* Changwoo Park, and Honglyoul Ju\**

J. Yoon, H. Kim, G. Lee, Prof. H. L. Ju

Department of Physics, Yonsei University, Seoul, 120-749, Republic of Korea

E-mail: [tesl@yonsei.ac.kr](mailto:tesl@yonsei.ac.kr)

Prof. X. Chen

Dept. of Mechanical and Aerospace Engineering, Hong Kong University of Science and Technology, Hong Kong

Dr. N. Tamura

Advanced Light Source, Lawrence Berkeley National Laboratory, Berkeley, USA

Prof. B. S. Mun

Department of Physics and Photon Science, Ertl Center for Electrochemistry and Catalysis, Gwangju and Institute of Science and Technology, Gwangju 500-712, Republic of Korea

E-mail: [bsmun@gist.ac.kr](mailto:bsmun@gist.ac.kr)

Prof. C. Park

Division of Applied Chemistry and Biotechnology, Hanbat National University, Daejeon 305-719 and Advanced Nano Products, Sejong 339-942, Republic of Korea

Keywords: vanadium dioxide, metal-insulator transition, phase transition temperature, phase transition speed, size effect, microcrystal, high-speed resistance

We investigate the control of two important parameters in VO<sub>2</sub> crystals - the temperature and speed of phase transition - by varying the crystal size. By decreasing the width of the square cylinder-shaped microcrystals from ~80 to ~1 μm, the phase transition temperature varies as much as 26.1 °C (19.7 °C) during heating (cooling) while the phase transition speed increases by a factor of 37 from  $4.6 \times 10^2$  to  $1.7 \times 10^4$  μm/s. The interplay between phase transition temperature and size of VO<sub>2</sub> microcrystals can be explained through the statistical behavior of first-order phase transition and size dependent thermal dissipation effect.

Among the many important materials for future industrial applications, VO<sub>2</sub> has received much attention due to not only the fascinating physical properties of a strongly correlated electron system, but also to its enormous potential for future technological applications.<sup>[1-11]</sup> At just above room temperature (~67 °C), VO<sub>2</sub> undergoes a first order metal-insulator transition (MIT) with a dramatic change in electrical resistance of 4 to 5 orders of magnitude.<sup>[2,3]</sup> Also, at the moment of the MIT, VO<sub>2</sub> undergoes a first order structural phase transition from a monoclinic to a rutile structure. One important aspect of the phase transition in VO<sub>2</sub> is that it can be induced by diverse methods other than thermal activation, such as the application of pressure,<sup>[4]</sup> light,<sup>[5,6]</sup> current,<sup>[7,8]</sup> and voltage.<sup>[9]</sup> Moreover, in the case of optically induced MIT, the transition occurs at an ultrafast time scale.<sup>[5,6]</sup> Consequently, these unique physical properties promote VO<sub>2</sub> as one of the best candidates for future advanced materials in a variety of applications fields, including ultrafast sensor,<sup>[10]</sup> optical switching devices,<sup>[11]</sup> memories,<sup>[12]</sup> tunable resonators,<sup>[13]</sup> and Mott transistors.<sup>[14]</sup> However, despite the tremendous recent advances in the fundamental understanding of the underlying physics of the MIT as well as in the engineering process for the utilization of VO<sub>2</sub> as practical devices, there are still many challenging tasks remaining for the implementation of VO<sub>2</sub> as a reliable material for commercial products. Especially, among the many critical tasks, the control of the phase transition temperature and speed has the highest priority as the scopes and functionalities of VO<sub>2</sub> applications strongly depend on these two parameters.

Over the years, many research groups have invested massive efforts not only to identify the origin of the phase transition in VO<sub>2</sub>, but also to control the occurrence of the phase transition onset by varying many physical parameters, such as doping,<sup>[15,16]</sup> strain,<sup>[17,18]</sup> pulsed voltage,<sup>[19,20]</sup> and size,<sup>[21-23]</sup> . It has been reported that the phase transition temperature

decreases by doping high valent ( $\geq 4+$ ) ions, e.g.  $W^{6+}$ ,  $Nb^{5+}$ ,  $Mo^{6+}$ , while the phase transition temperature increases with doping of trivalent ions, e.g.  $Cr^{3+}$ ,  $Fe^{3+}$ ,  $Ga^{3+}$ ,  $Al^{3+}$ .<sup>[15,16]</sup> Recently, Whittaker et al. reported that the phase transition temperature can be decreased by oxygen vacancy doping, which is induced by reducing  $VO_2$  crystal size to nanoscale.<sup>[22]</sup> Variations of crystal dimensions also provide a way to control the onset of the phase transition in  $VO_2$ . Previously, Lopez et al. reported the heterogeneous nature of the nucleation process and the possibility of increasing  $VO_2$  phase transition temperature by reducing dimensions using  $VO_2$  nano-particles embedded in  $SiO_2$  matrices.<sup>[21,24]</sup> These authors postulated that the defects in  $VO_2$  nano-particles can act as nucleation sites for the phase transition.

On the other hand, in solid-state physics, the spatial confinement of ordinary materials to ultra-small scale often leads to new physical phenomena. As semiconductors, such as Si,<sup>[25]</sup> Ge,<sup>[26]</sup> or CdSe,<sup>[27]</sup> are spatially confined below the exciton Bohr radius, quantum size effect occurs, i.e. the band gap of semiconductor increases with decreasing crystal size. In addition, various physical properties, e.g. structural strength,<sup>[28]</sup> magnetism,<sup>[29]</sup> ferroelectricity,<sup>[30]</sup> thermoelectric power,<sup>[31]</sup> are known to show dramatic changes as the dimensions of the material are reduced. In the case of  $VO_2$ , the probability of phase transition is expected to be strongly dependent on the size of the sample<sup>[21]</sup>. As the sample size decreases, the probability of phase transition decreases. Consequently, the onset temperature of phase transition of smaller samples is expected to increase (decrease) during heating (cooling) compared to larger samples. Moreover, the transition speed of  $VO_2$  is greatly limited by thermal dissipation conditions due to the exchange of the latent heat with the surrounding environment, showing that the effective surface areas for thermal interaction would become an important parameter for the transition speed in  $VO_2$ . That is, the interplay between size and effective surface area of  $VO_2$  are the important parameters for controlling phase transition properties.

In this report, we describe a systematic method to tune the phase transition temperature and its speed in VO<sub>2</sub> microcrystals by controlling size, greatly enhancing the potential of VO<sub>2</sub> for advanced devices. By varying the dimensions of the VO<sub>2</sub> microcrystals, we demonstrate that the onset temperature for phase transition can be varied from 67.4 up to 93.1 °C while the transition speed can be enhanced from  $4.6 \times 10^2$  μm/s up to  $1.7 \times 10^4$  μm/s. Using statistical behavior analysis of first-order phase transition with size dependent thermal dissipation effect, the correlation among phase transition temperature, speed, and the size of VO<sub>2</sub> microcrystals is investigated.

For the present study of the MIT size dependence in VO<sub>2</sub>, high-quality square cylinder-shaped VO<sub>2</sub> microcrystals are fabricated as shown in **Figure 1**. Free standing high quality VO<sub>2</sub> microcrystals with a square cross section and width ( $w$ ) ranging from ~1 to ~80 μm are prepared on an Al<sub>2</sub>O<sub>3</sub> boat by self-flux evaporation method. The details of the crystal elaboration process can be found elsewhere.<sup>[32]</sup> The microstructure and composition of VO<sub>2</sub> crystals were characterized by scanning electron microscopy (SEM) (JSM-7001F, JEOL). In Figure 1a-1c, a few selected SEM images of VO<sub>2</sub> microcrystals are shown, revealing the cross-section of the microcrystals to be almost square. In a previous report, we have shown that these high quality VO<sub>2</sub> single crystals show a heterogeneous first-order phase transition propagating from one end of the crystal surface to the other.<sup>[33]</sup> (also see Figure S1 and Video S1 in Supporting Information) Since few numbers of defects are present in these high-quality single crystals, the probability of phase transition initiating from a defect inside the crystal is assumed to be negligible.

Once the microcrystals are prepared, optical microscopy was employed to monitor the onset of phase transition in these VO<sub>2</sub> microcrystals.<sup>[33]</sup> Due to different optical reflectivity

between the metal and insulator phases in VO<sub>2</sub>, optical microscopy can provide direct real-time images of phase transition appearing on the surface of VO<sub>2</sub> during phase transition. Figure 1d-1e show optical microscope images of VO<sub>2</sub> microcrystal with length of 42 μm and width of 3.1 μm, just before and after the phase transition during heating, exhibiting single domain characteristics of phase transition without any complication of grain boundary and domain structure, i.e. we have either pure metallic or insulating single domain across the crystals. Previous synchrotron x-ray micro-diffraction results on identical microcrystals revealed that the growth direction (length direction) of VO<sub>2</sub> microcrystals is along the *c*-direction of the rutile phase (**c<sub>R</sub>**), [001].<sup>[32,33]</sup> The optical images of Figure 1d-1e are different from those of VO<sub>2</sub> nano-wires or thin films, where the metallic and insulating phases are shown together to coexist during phase transition.<sup>[17,18,34]</sup> In addition, the heterogeneous phase transition in these crystals occurs from the end surfaces and proceeds with phase boundary motion.<sup>[33]</sup> This is different from the recent report by Lopez et al.,<sup>[24]</sup> where MIT is initiated by heterogeneous nucleation at extrinsic defect sites within the crystal.

Next, the onset temperature of phase transition in VO<sub>2</sub> microcrystals is monitored as the size of crystal is varied, i.e. crystal width (*w*) from 1.9 to 77 μm. **Figure 2a** shows schematics of the experimental set-up for thermal optical microscopy on VO<sub>2</sub> microcrystals. As discussed in Figure S1, the phase transition of VO<sub>2</sub> occurs with phase boundary motion along the rutile *c*-axis and the propagation of MIT starts from one end of the microcrystals, suggesting the probability of the phase transition onset being linked to the end surface areas ( $2w^2$ ). In order to check this idea out, the onset temperature of MIT phase transition is plotted as a function of the width of microcrystal, *w*, as shown in Figure 2b. Interestingly, it can be seen that the phase transition temperatures rapidly increases (decreases) as the width of the crystal decreases in both the heating and cooling processes. In the case of the 3.6 μm thick

microcrystals, the onset temperature of phase transition is as high (low) as 93.1 °C (49.2 °C) during heating (cooling). This change in onset temperatures of phase transition is larger than those from doped VO<sub>2</sub> crystals, e.g. Cr, Fe, Ga, Al, by at most ~10 °C. <sup>[15,16]</sup> Also, the hysteresis, the difference of phase transition onset temperature between heating and cooling processes, increases as  $w$  decreases, e.g. the hysteresis of 3.6 μm thick crystal reached a value as large as 43.9 °C. The MIT temperature and hysteresis width of each measured samples are shown in Table S1.

To analyze the results of Figure 2, we applied the classical nucleation theory of phase transition. <sup>[35]</sup> In general, heterogeneous nucleation, i.e., the origin of phase transition onset in VO<sub>2</sub> occurs at preferential sites such as grain boundaries, surfaces, or intrinsic and extrinsic defects. In the case of high-quality single microcrystals, the preferential sites of nucleation are the two end surfaces and the nucleation starts at either one or both end surfaces. Since the effective surface energy at both end surfaces is believed to be lower than on the long side surfaces, the nucleation probability is expected to depend on both end surface area,  $S$  ( $= 2w^2$ ). If  $\rho$  is the density of suitable heterogeneous nucleating sites per unit surface, the probability of finding one nucleation site in a small area ( $dS$ ) at the end surface is defined by  $\rho dS$ . Since the probability is very small, the probability of occurrence of more than 2 sites is assumed to be negligible. Then, the probability,  $F$ , that the surface contains at least one nucleation site is  $F = 1 - \exp[-\rho S]$ . <sup>[35-37]</sup>

Now, in consideration of temperature contribution to the probability,  $\rho$  can be written as  $B\Delta g_{ex}^n$ , where  $B$  is a constant,  $n$  is an exponent and  $\Delta g_{ex}$  is the driving force of phase transition, i.e. the Gibbs free energy difference per unit volume between metal and

insulator phases.<sup>[24,37]</sup> If we further assume that phase transition occurs when  $F$  had the same (or most probable) probability regardless of size in Figure 2b,  $\rho S$  becomes a constant. Noting that  $\Delta g_{ex}$  is directly proportional to  $|T - T_c|$ ,  $\rho S = B \Delta g_{ex}^n S = C |T - T_c|^n S = D$ , where both  $C$  and  $D$  are constants.

Finally, by using the logarithm on both sides of the equation, we get  $\log \frac{1}{S} = n \log |T - T_c| + \log \frac{D}{C}$ . To test this derivation, the values of  $\log \frac{1}{S}$  and  $\log |T - T_c|$  are plotted together and a linear relationship is found as expected (shown in Figure 2c-d). The average value (66.6 °C) of phase transition temperature during heating (68.2 °C) and that of cooling (65.4 °C) for the largest crystal ( $w = 77 \mu m$ ) was used for the value of  $T_c$ . From the fitting of Figure 2c-2d,  $n$  and  $\log \frac{D}{C}$  values during heating (cooling) were obtained as  $1.6 \pm 0.4$  ( $1.9 \pm 0.3$ ) and  $-3.9 \pm 0.4$  ( $-3.9 \pm 0.2$ ). The exponent ( $\sim 1.9$ ) for the cooling side is practically the same as that ( $\sim 1.6$ ) of the heating side within experimental errors. These exponents may provide essential guidelines of any theoretical model for the nucleating defect creation. From the above discussion, MIT temperature of microcrystals during heating and cooling are given by  $T_+ = T_c (66.6 \text{ °C}) + 1.7 \times 10^2 \text{ °C} \left( \frac{1}{w(\mu m)} \right)^{1.2}$  and  $T_- = T_c (66.6 \text{ °C}) - 8.5 \times 10^1 \text{ °C} \left( \frac{1}{w(\mu m)} \right)^{1.1}$ , where “+” and “-” signs refer to the heating and cooling cycles, respectively. Hysteresis is given by  $\Delta T = T_+ - T_- = 1.7 \times 10^2 \text{ °C} \left( \frac{1}{w(\mu m)} \right)^{1.2} + 8.5 \times 10^1 \text{ °C} \left( \frac{1}{w(\mu m)} \right)^{1.1}$ . From this analysis, the hysteresis is expected to increase with the decrease of the crystal width. It predicts that  $T_-$  can be lower than room temperature when the width is below 1  $\mu m$ . In this case, hysteresis is expected to be

a large value of more than  $\sim 100$  °C. Large hysteresis is an important property of VO<sub>2</sub> based optical switches, memory, and related fields since it is related to the ability of maintaining stable phase under a large external impulse.

As the sample size shows a close relation with phase transition temperature, the size effect on phase transition speed is investigated next. Since our microcrystals display the onset of phase transition with the propagation of phase boundary from one end to the other, the speed of the phase boundary during MIT, i.e. phase transition speed, can be estimated from the measurements of crystal length and the propagation time of the phase boundary. To monitor the propagation time and the phase transition speed, the high speed resistance of the VO<sub>2</sub> crystals is measured using a dc two-contact four-probe method, shown in **Figure 3a**. The details of photolithography process for resistance measurement of VO<sub>2</sub> microcrystals are described in Figure S2. High-speed resistance measurements collecting data at a rate up to 5,000 per second are carried out with a source meter (Keithley 2611A). Though the onset of MIT and its propagation along long ( $> \sim 200$   $\mu\text{m}$ ) samples can be observed under optical microscope, the same measurement becomes difficult for short samples with length  $< \sim 200$   $\mu\text{m}$  due to fast MIT and limited shutter speed of CCD camera for a given sample size. Indeed, the CCD camera attached to the optical microscope can only take up to 60 frames per second or  $\sim 17$  ms between images. Figure 3b shows one of measurements of the temperature dependence of the resistance from a VO<sub>2</sub> crystal with width of 1.9  $\mu\text{m}$ . The inset of Figure 3b shows the optical image of the crystal with Au (1000nm)/Cr(10 nm) electrical contacts for the widths of the 1.9  $\mu\text{m}$  taken during the resistance measurements. The VO<sub>2</sub> crystal shows sharp phase transition with a rectangular shape hysteresis loop. The temperature dependences of the resistance curves with different widths were measured. (Figure S3 and Table S2 in Supporting Information) The MIT onset temperature from the resistance measurement during heating is in the range of  $\sim 62$  to

~67 °C, which is significantly lower than those observed in optical microscopy measurements. Based on the resistance curve in the temperature range of 50 - 60 °C in Figure 3b, the band gap,  $E_g$ , of VO<sub>2</sub> is calculated as 0.6 - 0.7 eV if VO<sub>2</sub> is assumed to be an intrinsic semiconductor.<sup>[38]</sup> These calculated band gaps are in good agreement with the previously reported values of 0.7 eV.<sup>[39,40]</sup> Also, the crystal structures before and after MIT onset, shown in Figure S4, are confirmed by synchrotron Laue microdiffraction to be the M2 and R phases, respectively.

Figure 3c displays the high-speed resistance measurement of VO<sub>2</sub> crystals during MIT with widths of 1.9 μm shown in Figure 3b during MIT under heating. (Also see Figure S5 in Supporting Information) As seen from the Figure 3c, during MIT, the resistance decreases at almost constant rate, which is in agreement with phase boundary motion. The phase transition time is defined as the time required for phase boundary to travel from one contact to the other ( $= \frac{l}{v}$ ), where  $l$  and  $v$  are the length between electrical contacts and phase boundary speed, respectively. Phase transition time drops rapidly from ~1 s to ~3 ms as the width ( $w$ ) of the microcrystal reduces from 40 to 1.9 μm, i.e., the speed increases rapidly with decreasing width of the microcrystal. Figure 3d shows crystal width dependence of the phase boundary speed during heating and cooling. While the speed of large crystals ( $w = 40 \mu\text{m}$ ) is  $4.6 \times 10^2 \mu\text{m/s}$ , the speed of smaller crystals ( $w = 1.9 \mu\text{m}$ ) is as high as  $1.7 \times 10^4 \mu\text{m/s}$ , which is almost 37 times faster than that of the large crystals. The width dependence of the phase boundary speed can be well fitted as an inverse function of the width,  $v(\mu\text{m/s}) = \frac{a}{w(\mu\text{m})}$ , with  $a = (3.3 \pm 0.1) \times 10^4 \mu\text{m}^2/\text{s}$  ( $a = (3.8 \pm 0.2) \times 10^4 \mu\text{m}^2/\text{s}$ ) during heating (cooling). Assuming the fitting results are valid for width down to 0.01 μm, the limit of linear plot in Figure 4d, then the speed during heating is expected to be  $3.3 \times 10^6 \mu\text{m/s}$  for that width. That is, the on/off

switch based on phase transition in VO<sub>2</sub> can be as fast as ~10 ns for a 10 nm wide, 30 nm long crystal, and this ultrafast phase boundary speed can be applied to the switching time of future VO<sub>2</sub> devices.

It is important to understand why the transition speed shows a  $\frac{1}{w}$  dependence in Figure 3d. There are several parameters that can be suspected to play a role in transition speed, such as the Gibbs free energy, Joule heating, electric field, and thermal dissipation. First, let's consider the Gibbs free energy. The transition temperatures from high speed resistance measurements are in the range of ~62 to 67 °C (~50 to 57 °C) during heating (cooling). If the Gibbs free energy plays a major role, the phase boundary speed is expected to increase as the Gibbs free energy increases with increasing  $|T - T_C|$ . Thus, during heating, the crystal with the higher phase transition temperature should have the higher speed. As shown in Table S2, the crystal with  $w = 40 \mu\text{m}$  has phase transition temperature of 66.3 °C, which is higher than either those (~62 °C) of the smaller crystals ( $w = 2.5$  and  $4.1 \mu\text{m}$ ). Thus the crystal with  $w = 40 \mu\text{m}$  is expected to have much larger speed than those crystals with  $w = 2.5$  and  $4.1 \mu\text{m}$ . However, the crystal with  $w = 40 \mu\text{m}$  has the lowest speed among those crystals. Since the transition speed does not show significant dependence on the magnitude of  $|T - T_C|$ , we conclude that the effect of driving force or the Gibbs free energy on the MIT speed is small.

Next, we examined the effect of Joule heating (current) and the magnitude of electric field on MIT speed. We measured the MIT speed with currents of 0.1 and 1  $\mu\text{A}$ , thus the current and the magnitude of the electric field are varied simultaneously by a factor of 10. [Figure S7 in Supporting Information] The phase boundary speeds of 0.1 and 1  $\mu\text{A}$  are found to have practically the same value of  $1.5 \times 10^4 \mu\text{m/s}$ . If either Joule heating or the magnitude of the

electric field plays a critical role in the transition speed, the transition speed should vary considerably as Joule heating and the magnitude of the electric field in the crystal differs significantly. However, the speeds in both cases are almost identical, which indicates that the dependence of the speed on either the magnitude of current or the magnitude of the electric field is small.

Finally, we examine the possibility that the size dependence of the phase transition speed originates from size-dependent thermal dissipation. First, we assume that the thermal time constant of the crystal is roughly the same as that of uniformly heated square cylinder. [Supporting Information] Thermal time constant  $\tau$  can be viewed as build-up times necessary for the onset of a heat flux after a temperature gradient is imposed on a given sample. The  $\tau$  of uniformly heated square cylinder is given by  $\tau = \frac{A}{\rho V c}$ , where  $A$ ,  $\rho$ ,  $V$ , and  $c$  are total bottom surface area, density, total volume, and heat capacity of unit mass of the cylinder. [Supporting Information] In the case of a square cylinder,  $A = lw$  and  $V = lw^2$ . The time constant becomes  $\tau = \frac{\rho w c}{\kappa} \propto w$ , where  $\rho$  is the density of VO<sub>2</sub>. That is, the thermal constant ( $\tau$ ) is linearly proportional to the width ( $\tau \propto w$ ), whose dependence originates from the increasing surface to volume ratio ( $\sim 1/w$  for square cylinders) with decreasing size. So the smaller crystal has the shorter time constant. In rough approximation, the time constant  $\tau$  is the same than the phase transition time. Thus the phase transition speed is roughly equal (or proportional to)  $\frac{l}{\tau}$ , and the speed depends on  $\frac{1}{w}$ , as observed. Since we observe the same dependence of thermal constant and transition speed, we believe the two have the same physical origin of a thermal dissipation mechanism.

In summary, the control of metal insulator phase transition temperature and transition speed is investigated with high-speed resistance measurement and optical microscopy. With the statistical description for a heterogeneous nucleation process, it is shown that the phase transition probability of VO<sub>2</sub> depends on the end surface width, and in turn the phase transition temperature varies as size gets modified. The variation of phase transition speed with sample size is explained with effective thermal exchange process of surface to volume ratio. We conclude, therefore, that the onset of MIT and the MIT speed can be finely and effectively tuned by controlling the crystal size.

### **Supporting Information**

Supporting Information is available from the Wiley Online Library or from the author

### **Acknowledgements**

H. L. Ju and B. S. Mun would like to thank the Basic Science Research Program for support through the National Research Foundation of Korea (NRF) funded by the Korean Government (MOE) (2012R1A1A2006948 & 2012R1A1A2001745). B. S. Mun would like to thank the support from SRC and GIST College's 2015 TBP Research Fund. H. L. Ju thanks Yonsei University for financial support during 2015 sabbatical leave. The Advanced Light Source is supported by the Director, Office of Science, Office of Basic Energy Sciences, Materials Science Division, of the U.S. Department of Energy under Contract No. DE-AC02-05CH11231 at Lawrence Berkeley National Laboratory.

## Reference

- [1] Z. Yang, C. Ko, S. Ramanathan, *Annu. Rev. Mater. Res.* **2011**, *41*, 337.
- [2] F. J. Morin, *Phys. Rev. Lett.* **1959**, *3*, 34.
- [3] D. H. Kim, H. S. Kwok, *Appl. Phys. Lett.* **1994**, *65*, 3188.
- [4] E. Arcangeletti, L. Baldassarre, D. Di Castro, S. Lupi, L. Malavasi, C. Marini, A. Perucchi, P. Postorino, *Phys. Rev. Lett.* **2007**, *98*, 196406.
- [5] A. Cavalleri, C. Toth, C. W. Siders, J. A. Squier, F. Raksi, P. Forget, J. C. Kieffer, *Phys. Rev. Lett.* **2001**, *87*, 237401
- [6] C. Kübler, H. Ehrke, R. Huber, R. Lopez, A. Halabica, R. F. Haglund, A. Leitenstorfer, *Phys. Rev. Lett.* **2007**, *99*, 116401.
- [7] H.-T. Kim, B.-G. Chae, D.-H. Youn, S.-L. Maeng, G. Kim, K.-Y. Kang, Y.-S. Lim, *New J. Phys.* **2004**, *6*, 52.
- [8] A. Tselev, J. D. Budai, E. Strelcov, J. Z. Tischler, A. Kolmakov, S. V. Kalinin, *Nano Lett.* **2011**, *11*, 3065.
- [9] G. Stefanovich, A. Pergament, D. Stefanovich, *J. Phys.: Condens. Matter* **2000**, *12*, 8837.
- [10] E. Strelcov, Y. Lilach, A. Kolmakov, *Nano Lett.* **2009**, *9*, 2322.
- [11] Y. Gao, H. Luo, Z. Zhang, L. Kang, Z. Chen, J. Du, M. Kanehira, C. Cao, *Nano Energy* **2012**, *1*, 221.
- [12] M. J. Lee, Y. Park, D. S. Suh, E. H. Lee, S. Seo, D. C. Kim, R. Jung, B. S. Kang, S. E. Ahn, C. B. Lee, D. H. Seo, Y. K. Cha, I. K. Yoo, J. S. Kim, B. H. Park, *Adv. Mater.* **2007**, *19*, 3919.
- [13] a) M. Liu, H. Y. Hwang, H. Tao, A. C. Strikwerda, K. Fan, G. R. Keiser, A. J. Sternbach, K. G. West, S. Kittiwatanakul, J. Lu, S. A. Wolf, F. G. Omenetto, X. Zhang, K. A. Nelson, R. D. Averitt, *Nature* **2012**, *487*, 345; b) M. J. Dicken, K. Aydin, I. M. Pryce, L. A. Sweatlock, E. M. Boyd, S. Walavalkar, J. Ma, H. A. Atwater, *Opt. Express* **2009**, *17*, 18330.

- [14] S. Hormoz, S. Ramanathan, *Solid-State Electron.* **2010**, *54*, 654.
- [15] S. Zhang, I. S. Kim, L. J. Lauhon, *Nano Lett.* **2011**, *11*, 1443.
- [16] S. Lee, C. Cheng, H. Guo, K. Hippalgaonkar, K. Wang, J. Suh, K. Liu, J. Wu, *J. Am. Chem. Soc.* **2013**, *135*, 4850.
- [17] J. Wei, Z. H. Wang, W. Chen, D. H. Cobden, *Nature Nanotechnol.* **2009**, *4*, 420.
- [18] J. Cao, E. Ertekin, V. Srinivasan, W. Fan, S. Huang, H. Zheng, J. W. L. Yim, D. R. Khanal, D. F. Ogletree, J. C. Grossman, J. Wu, *Nature Nanotechnol.* **2009**, *4*, 732.
- [19] T. Driscoll, H.-T. Kim, B.-G. Chae, B.-J. Kim, Y.-W. Lee, N. M. Jokerst, S. Palit, D. R. Smith, M. Di Ventra, D. N. Basov, *Science* **2009**, *325*, 1518.
- [20] S.-H. Bae, S. Lee, H. Koo, L. Lin, B. H. Jo, C. Park, Z. L. Wang, *Adv. Mater.* **2013**, *25*, 5098.
- [21] R. Lopez, L. C. Feldman, R. F. Haglund, *Phys. Rev. Lett.* **2004**, *93*, 177403.
- [22] L. Whittaker, C. Jaye, Z. Fu, D. A. Fischer, S. Banerjee, *J. Am. Chem. Soc.* **2009**, *131*, 8884.
- [23] L. Hongwei, L. Junpeng, Z. Minrui, T. S. Hai, S. C. Haur, Z. Xinhai, K. Lin, *Opt. Express* **2014**, *22*, 30748.
- [24] R. Lopez, T. E. Haynes, L. A. Boatner, L. C. Feldman, R. F. Haglund, *Phys. Rev. B* **2002**, *65*, 224113.
- [25] Y. Hu, H. O. H. Churchill, D. J. Reilly, J. Xiang, C. M. Lieber, C. M. Marcus, *Nature Nanotechnol.* **2007**, *2*, 622.
- [26] M. V. Wolkin, J. Jorne, P. M. Fauchet, G. Allan, C. Delerue, *Phys. Rev. Lett.* **1999**, *82*, 197.
- [27] C. R. Kagan, C. B. Murray, M. Nirmal, M. G. Bawendi, *Phys. Rev. Lett.* **1996**, *76*, 1517.
- [28] Z. P. Bažant, J.-L. Le, M. Z. Bazant, *Proc. Natl. Acad. Sci. U.S.A.* **2009**, *106*, 11484.
- [29] Y.-W. Jun, Y.-M. Huh, J.-S. Choi, J.-H. Lee, H.-T. Song, S. Kim, S. Yoon, K.-S. Kim, J.-

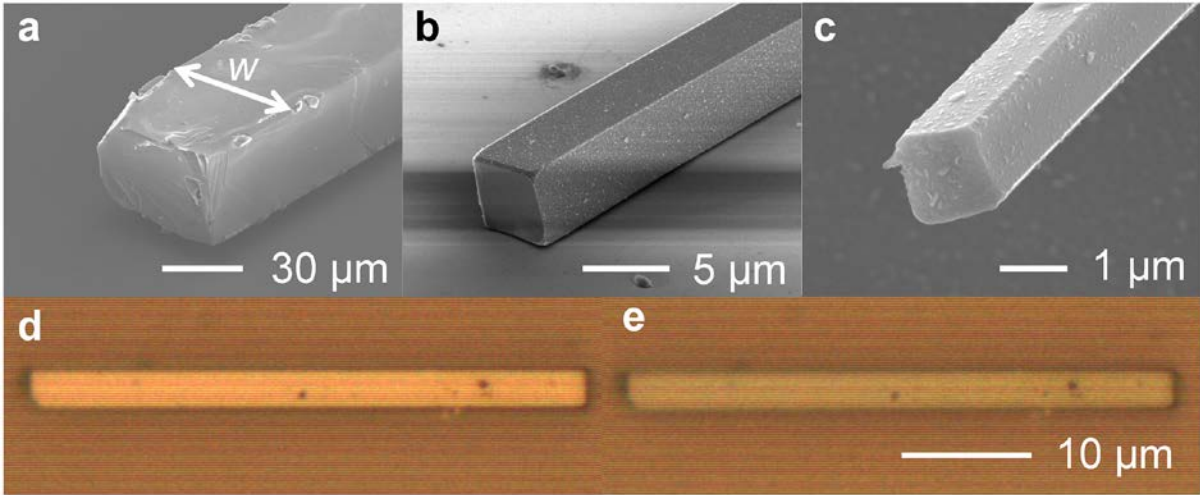
- S. Shin, J.-S. Suh, J. Cheon, J. Am. Chem. Soc. **2005**, *127*, 5732.
- [30] K. Ishikawa, K. Yoshikawa, N. Okada, Phys. Rev. B **1988**, *37*, 5852.
- [31] M. S. Dresselhaus, G. Chen, M. Y. Tang, R. G. Yang, H. Lee, D. Z. Wang, Z. F. Ren, J. P. Fleurial, P. Gogna, Adv. Mater. **2007**, *19*, 1043.
- [32] B. S. Mun, K. Chen, Y. Leem, C. Dejoie, N. Tamura, M. Kunz, Z. Liu, M. E. Grass, C. Park, J. Yoon, Y. Y. Lee, H. Ju, Phys. Status Solidi RRL **2011**, *5*, 107.
- [33] B. S. Mun, K. Chen, J. Yoon, C. Dejoie, N. Tamura, M. Kunz, Z. Liu, M. E. Grass, S.-K. Mo, C. Park, Y. Y. Lee, H. Ju, Phys. Rev. B **2011**, *84*, 113109.
- [34] M. M. Qazilbash, M. Brehm, B. G. Chae, P. C. Ho, G. O. Andreev, B. J. Kim, S. J. Yun, A. V. Balatsky, M. B. Maple, F. Keilmann, H. T. Kim, D. N. Basov, Science **2007**, *318*, 1750.
- [35] D. A. Porter, K. E. Easterling, M. Y. Sherif, *Phase Transformations in Metals and Alloys*, CRC Press, Boca Raton, FL, 2009
- [36] J. E. Freund and R. E. Walpole, *Mathematical Statistics*, Prentice-Hall, Englewoods Cliffs, NJ, 1987.
- [37] I.-W. Chen, Y.-H. Chiao, and K. Tsukazi, Acta Metall. **1985**, *33*, 1847.
- [38] J.S. Blackmore, *Semiconductor Statistics*, Pergamon Press, Oxford, 1962.
- [39] D. Brassard, S. Fourmaux, M. Jean-Jacques, J. C. Kieffer, M.A. El Khakani, Appl. Phys. Lett. **2005**, *87*, 051910.
- [40] W. Liu, J. Cao, W. Fan, Z. Hao, M. Martin, Y. R. Shen, J. Wu, and F. Wang, Nano Lett. **2011**, *11*, 466.

## Figure Captions

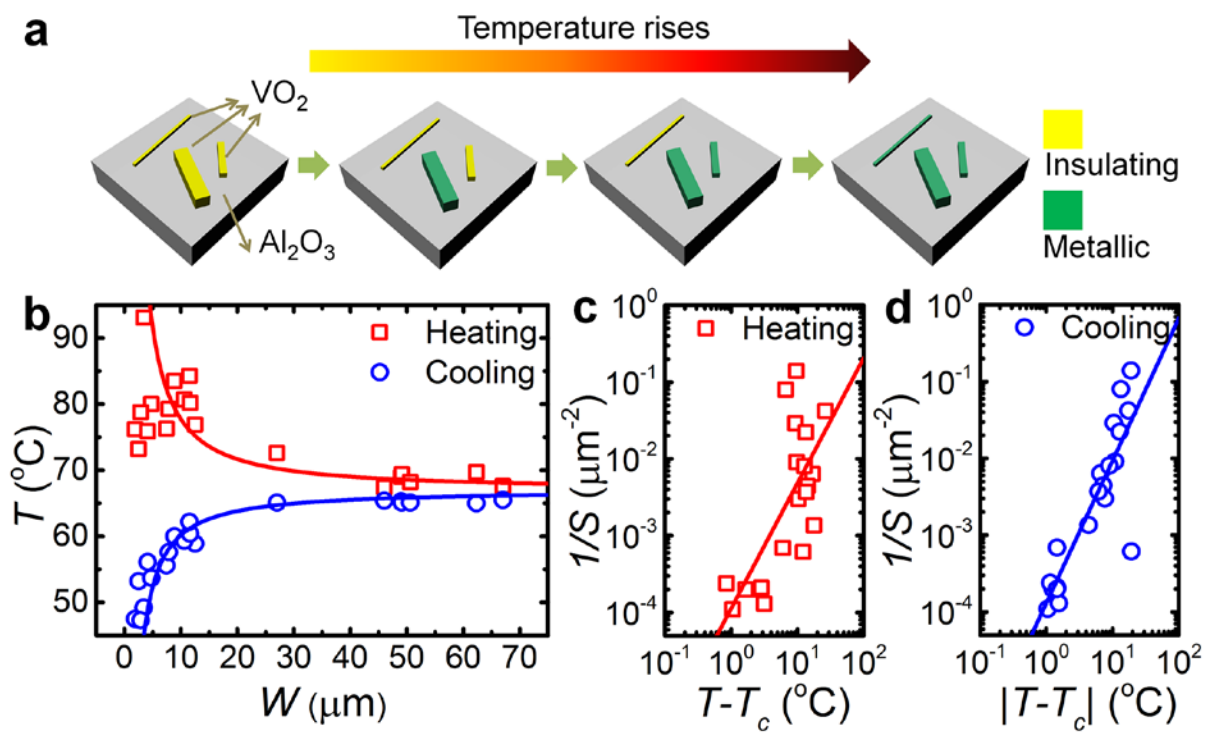
Figure 1. Scanning electron microscope image of a square cylinder shape VO<sub>2</sub> microcrystal with width of (a) 67 μm, (b) 4.3 μm, and (c) 1.3 μm. Optical microscope images of the small VO<sub>2</sub> microcrystal with width 3.1 μm and length 42 μm, just (d) before and (e) after the MIT.

Figure 2 (a) Schematic drawing of crystal size dependence of the MIT temperature of VO<sub>2</sub> microcrystals. The smaller crystal tends to have the higher transition temperature due to the smaller probability of the phase transition. (b) Dependence of the MIT temperature on crystal size (width) during heating (empty red square) and cooling (empty blue circle). The inverse of end surface area  $\frac{1}{S}$  versus the difference in the MIT temperature  $|T - T_c|$  curve of VO<sub>2</sub> microcrystals on (c) heating and (d) cooling.

Figure 3 (a) The schematic of the patterned crystal sample circuit geometry with Au (1000 nm)/Cr(10 nm) contacts used for the high speed and temperature dependence of the resistance measurements. (b) Temperature dependence of the resistance of VO<sub>2</sub> crystal with widths of 1.9 μm. Inset shows an optical microscope image of the VO<sub>2</sub> crystal used for the resistance measurement. (c) High speed resistance measurement of VO<sub>2</sub> crystal in (b). Insets show schematics of the phase boundary motion during MIT. (d) Dependence of the phase boundary speed ( $v$ ) on crystal width ( $w$ ) during heating (empty red square) and cooling (empty blue square).



**Figure 1**



**Figure 2**

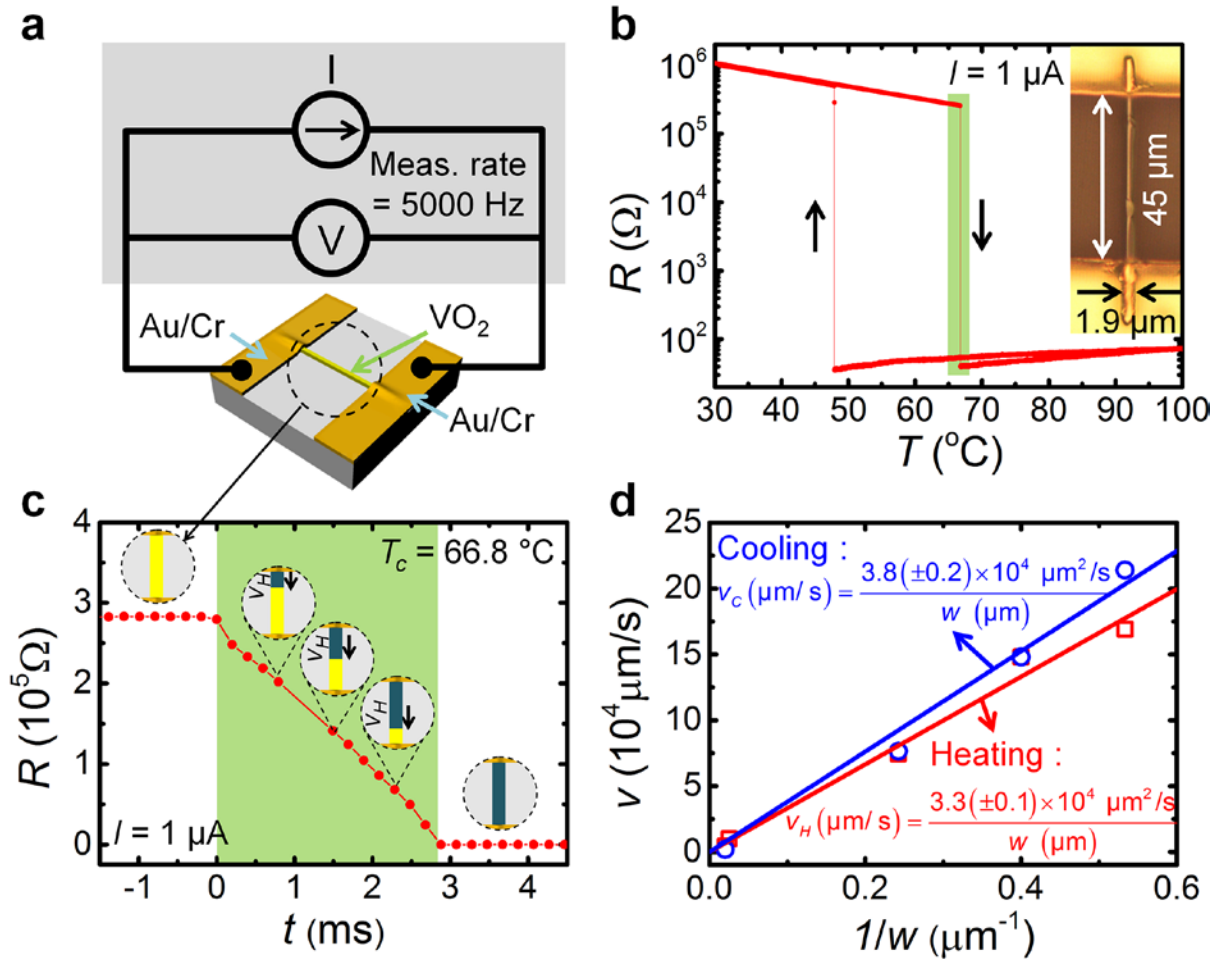


Figure 3